

Synthesis of Second-Generation Transition State Analogues of Human Purine Nucleoside Phosphorylase

Gary B. Evans,^{*,†} Richard H. Furneaux,[†] Andrzej Lewandowicz,[‡] Vern L. Schramm,[‡] and Peter C. Tyler[†]

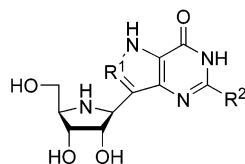
Carbohydrate Chemistry Team, Industrial Research Limited, P.O. Box 31310, Lower Hutt, New Zealand, and Department of Biochemistry, Albert Einstein College of Medicine of Yeshiva University, 1300 Morris Park Avenue, Bronx, New York 10461

Received June 24, 2003

Purine nucleoside phosphorylases (PNPs) catalyze nucleophilic displacement reactions by migration of the cationic ribooxacarbenium carbon between the fixed purine and phosphate nucleophiles. As the phosphorolysis reaction progresses along the reaction coordinate, the distance between the purine and carbocation increases and the distance between carbocation and phosphate anion decreases. Immucillin-H and Immucillin-G have been shown previously to be potent inhibitors of PNP. We now report the synthesis of a second generation of stable transition state analogues, DADMe-Immucillins **2**, **3**, and **4**, with increased distance between ribooxacarbenium and purine mimics by incorporation of a methylene bridge between these groups. These compounds are potent inhibitors with equilibrium dissociation constants as low as 7 pM against human PNP. Stable chemical analogues of enzymatic transition states are necessarily imperfect since they lack the partial bond character of the transition state. The immucillins and DADMe-Immucillins represent approaches from the product and reaction side of the transition state.

Introduction

Recently we reported the design,^{1–3} synthesis,^{4–6} and biological activity of the Immucillins, a series of high affinity transition state analogue inhibitors of bovine,^{7–10} malarial,^{11,12} *Mycobacterium tuberculosis*,^{13,14} and human PNPs (purine nucleoside phosphorylases).^{7,15} In humans, a genetic deficiency in PNP leads to a build-up of deoxyguanosine triphosphate (dGTP) in human T-cells and results in cell death for proliferating T-cells. The human T-cell is unique in this regard because of a combination of high deoxycytidine kinase activity (which phosphorylates deoxyguanosine) and a relatively low nucleotidase activity which allows dGTP to accumulate.^{16,17} The implication has been^{18,19} that inhibition of PNP provides a mechanism to suppress T-cell proliferation in human beings and this prediction is being borne out in human clinical studies using Immucillin-H (as BCX-1777).²⁰ Perturbation of T-cell population through the inhibition of PNP provides new avenues for the treatment of T-cell-mediated disorders.¹⁹



R¹=CH, R²=H Immucillin-H

R¹=CH, R²=NH₂ Immucillin-G

R¹=N, R²=H 8-Aza-Immucillin-H

The transition state structures for the bovine PNP-catalyzed phosphorolysis of inosine have been solved by

* Corresponding author. Fax +64-4-9313055; e-mail g.evans@irl.cri.nz.

[†] Industrial Research Limited.

[‡] Albert Einstein College of Medicine of Yeshiva University.

kinetic isotope effects (Figure 1). The characteristics of the transition state, i.e., the ribooxacarbenium ion character in the ribosyl group and the elevated pK_a for the purine-leaving group with little participation of the phosphate ion, have been partially captured by the Immucillins. To better mimic the cationic charge which develops at the anomeric carbon and the dissociative transition state, we designed DADMe-Immucillin-H in which the nitrogen atom is now at the anomeric carbon, the ring oxygen is replaced with a methylene group, and the ribosyl mimic and the deazapurine have increased separation through insertion of a methylene bridge.

In a recent publication we described the potent inhibition of *Mycobacterium tuberculosis* PNP²¹ by the second-generation versions of the Immucillins, the DADMe-Immucillins. The DADMe-Immucillins mimic structures further along the phosphorolysis reaction coordinate than the Immucillins. We report here the first synthesis of the DADMe-Immucillins **2**, **3**, and **4** and their activity against human PNP.

Results and Discussion

Synthesis. The 1'-aza sugar (3*R*,4*R*)-3-hydroxy-4-(hydroxymethyl)pyrrolidine (**1**) was first reported by Jaeger and Biel as a mixture of stereoisomers.²² Bols et al. reported the enzymatic chiral resolution of racemic 3,4-*trans*-3-hydroxy-4-(hydroxymethyl)pyrrolidine²³ and the first asymmetric synthesis of **1** was reported by Ichikawa et al.²⁴ We prepared **1** by a modification of the method of Filichev and Pedersen in 12 steps from D-xylose,²⁵ in which **5** was protected by *tert*-butoxycarbonylation to afford **6**, rather than Fmoc protection (Scheme 1). Periodate cleavage of compound **6** followed by reduction of the resulting aldehyde with sodium borohydride yielded (3*R*,4*R*)-*N*-*tert*-butoxycarbonyl-3-hydroxy-4-hydroxymethylpyrrolidine (**7**). Protection of the hydroxyl groups of **7** was effected by treatment with

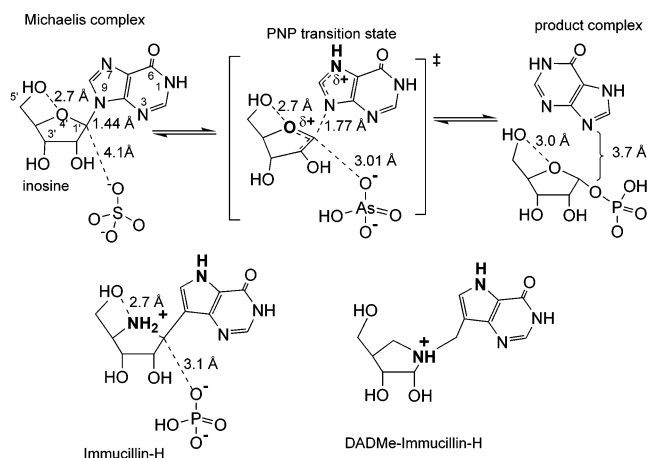


Figure 1. Phosphorolysis of inosine catalyzed by PNP with features of the transition state and selected features for the Michaelis complexes.

sodium hydride and benzyl bromide to afford the dibenzyl ether **8**. Deprotection of compounds **7** and **8** could be achieved by treatment with concentrated hydrochloric acid in methanol to afford hydrochloride salts **1** and **9**, respectively.

Initially, attempts were made to construct the deazapurines via the de novo approach first published by Kline et al.^{26–28} and adapted by ourselves to synthesize the Immucillins,⁵ which starts by constructing the propionitrile adduct **10** (Scheme 2). However on attempted reaction with either Bredereck's reagent or ethyl formate and sodium hydride **10** reverted to **9** as the free base, presumably via β elimination. Therefore alternative routes to the desired compounds were investigated.

The reductive aminations of the hydrochloride salts of **1** or **9** with an appropriately formylated deazapurine were investigated, as the convergent nature of this reaction was attractive. Formylation of the previously reported bromodeazapurines compounds **11**,¹⁵ **12**,²⁹ and **13**³⁰ was achieved via lithium–halogen exchange to afford the formyl derivatives **14**, **15**, and **16**, respectively, in good yields (Scheme 3).

With the formyl group in place, we investigated the coupling of these compounds to the dibenzyl ether **9** and (3*R*,4*R*)-3-hydroxy-4-(hydroxymethyl)pyrrolidine (**1**) itself by reductive amination. The protected amine hydrochloride **9** was allowed to react with aldehyde **14** in the presence of sodium cyanoborohydride in methanol to afford **17** as the sole product in good yield (Scheme 4). Removal of the *tert*-butyl protecting group of compound **17** using TFA in DCM yielded **18**. Similarly, the amine hydrochloride **1** reacted with aldehydes **14** and **16** under the same conditions to afford the corresponding protected DADMe-Immucillins **19** and **20**, respectively.

Deprotection could be achieved via treatment with concentrated hydrochloric acid in methanol at reflux, or in the case of compound **20** at room temperature, to afford compounds **2**, **3**, and **4**, (Scheme 5).

Improved yields of DADMe-Immucillin-H (**2**) were achieved via the mild acid hydrolysis of the *tert*-butyl group followed by catalytic hydrogenolysis of the remaining benzyl groups and subsequent treatment with

aqueous ammonia to remove the remaining N-7 hydroxymethyl residue.

Inhibition of Purine Nucleoside Phosphorylase by DADMe-Immucillins. The human genetic deficiency of PNP causes a specific T-cell immunodeficiency.³¹ Pharmacologic intervention in T-cell proliferation is desirable in T-cell cancers, autoimmune diseases, and tissue transplant rejection.¹⁸ The first generation PNP inhibitor Immucillin-H is in clinical trials against T-cell cancers.²⁰ Experiments with xenograft models with mice have established that Immucillin-H is as effective as cyclosporin in mouse models of tissue transplant rejection and that combinations of Immucillin-H and cyclosporin are more effective than each individual agent.³² Pharmacokinetic studies indicate that immunological, anticancer, and pharmacokinetic properties of anti-PNP agents will be key to their development as anticancer and autoimmune agents.³³

Biological effectiveness of anti-PNP agents *in vivo* depends on the complete inhibition of the target enzyme. Therefore inhibitors with even higher specificity and affinity than the Immucillins remain attractive targets. The first generation inhibitors Immucillin-H, Immucillin-G, and 8-Aza-Immucillin-H are 56, 42, and 180 pM inhibitors, respectively, for the human enzyme^{7,8} whereas DADMe-Immucillin-H (**2**), DADMe-Immucillin-G (**3**), and 8-Aza-DADMe-Immucillin-H (**4**) are 16, 7, and 2000 pM inhibitors of human PNP, respectively (Table 1).

Compared to Immucillin-H, the current clinical agent, DADMe-Immucillin-G (**3**), exhibits an approximately 8-fold increase in affinity. 8-Aza-DADMe-Immucillin-H (**4**) is a less potent inhibitor than 8-Aza-Immucillin-H.

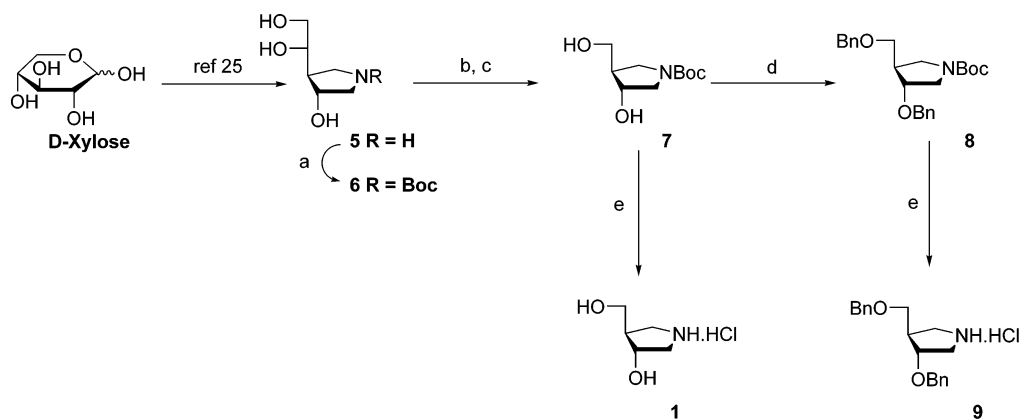
Administration of tight-binding transition state analogues as pharmacophores has the potential to target the enzyme of interest with high specificity. The biological half-life is closely related to the residence time on the catalytic site of the target enzyme. Residence time is dominated by the off-rate, although on-rates can also contribute.³⁴ The increased affinity of DADMe-Immucillin-G (**3**) is highly significant in terms of pharmacology. It implies an 8-fold increased time for biological effectiveness and therefore an 8-fold change in dose scheduling. Finally, the DADMe-Immucillins have only two asymmetric centers compared to the four centers in Immucillin-H. This is expected to improve the synthetic efficiency for these potential anti-T-cell agents.

Conclusions

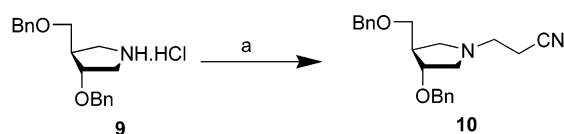
This report establishes that extended geometry for transition state analogue of PNP can more efficiently capture the features of the transition state for human PNP. Immucillin-H is a substrate-like transition state mimic while DADMe-ImmH is more closely related to products. The significance of this knowledge is that relatives of both early and late transition state analogues can now be explored in attempts to ascend higher on the slopes toward the transition state. Both inhibitors are efficient analogues in the specific case of PNP. The K_m for the human enzyme described here is 38 μ M, giving a K_m/K_i^* ratio for Immucillin-H and DADMe-Immucillin-G of 679 000 and 5 590 000, respectively.

Experimental Section

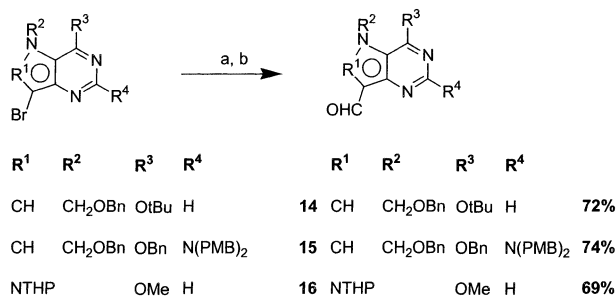
General. NMR spectra were recorded on a Bruker AC-300 instrument at 300 MHz (¹H) or 75 MHz (¹³C). Normally, spectra were measured in CDCl₃ with Me₄Si as internal

Scheme 1^a

^a Reagents: (a) Boc_2O , MeOH, room temp., 73%; (b) NaIO_4 , EtOH, 0 °C; (c) NaBH_4 , EtOH, 0 °C, 92% for two steps; (d) BnBr, NaH, DMF, 0 °C, 96%; (e) MeOH, HCl , room temp, quantitative.

Scheme 2^a

^a Reagents: (a) 3-Bromopropionitrile, Hunigs base, acetonitrile, room temp.

Scheme 3^a

^a Reagents: (a) $t\text{BuLi}$, THF, -78 °C; (b) DMF, -78 °C, room temp.

reference; when D_2O was the solvent, acetone (δ ¹H, 2.20; ¹³C, 33.2) was used as an internal reference. High-resolution accurate mass determinations were performed by Hort Research Ltd., Palmerston North, N. Z., on a VG70-250S double focusing, magnetic sector mass spectrometer under chemical ionization conditions using isobutane or ammonia as the ionizing gas, or under high-resolution FAB conditions in a glycerol or nitrobenzyl alcohol matrix. Melting points were determined on a Reichert hot stage microscope and are uncorrected. Aluminum-backed silica gel sheets (Merck or Reidel de Haen) were used for thin-layer chromatography. Column chromatography was performed on silica gel (230-400 mesh, Merck). Chromatography solvents were distilled prior to use.

Chemistry. (3*R*,4*S*)-*N*-*tert*-Butoxycarbonyl-4-[(1*S*)-1,2-dihydroxyethyl]-3-hydroxypyrrolidine (**6**). Di-*tert*-butyl dicarbonate (4.54 g, 20.8 mmol) was added portionwise to a stirred solution of (3*R*,4*S*)-4-[(1*S*)-1,2-dihydroxyethyl]-3-hydroxypyrrolidine²⁵ (2.80 g, 18.9 mmol) in methanol at room temp. On complete addition the reaction was then left for 1 h and concentrated in vacuo. Chromatography afforded (3*R*,4*S*)-*N*-*tert*-butoxycarbonyl-4-[(1*S*)-1,2-dihydroxyethyl]-3-hydroxypyrrolidine (**6**) (3.4 g, 73%). ¹H NMR δ 4.36 (q, J = 7.5 Hz, 1H), 3.73-3.54 (m, 6H), 3.18-3.04 (m, 2H), 2.15 (brs, 1H), 1.45 (s, 9H). ¹³C NMR (many of the peaks are doubled due to slow interconversion of rotamers) δ 154.8, 80.0, 73.2 and 72.9, 72.4

and 71.4, 65.4, 52.1 and 51.7, 48.0 and 47.4, 46.7 and 46.3, 28.5. HRMS ($M-H^-$) calcd for $\text{C}_{11}\text{H}_{20}\text{NO}_5$: 2246.1341. Found 246.1348.

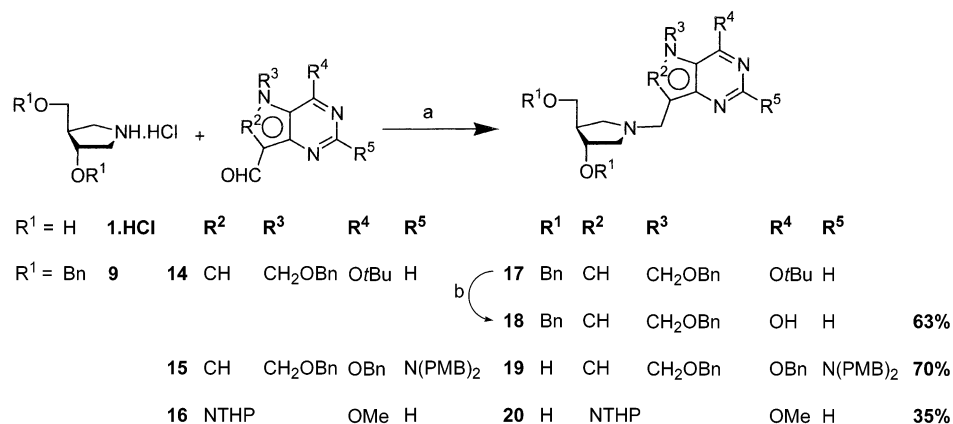
(3*R*,4*R*)-*N*-*tert*-Butoxycarbonyl-3-hydroxy-4-hydroxymethylpyrrolidine (**7**). (3*R*,4*S*)-*N*-*tert*-Butoxycarbonyl-3-hydroxy-4-[(1*S*)-1,2-dihydroxyethyl]pyrrolidine (**6**) (3.4 g, 13.7 mmol) in ethanol (50 mL) was added dropwise to a stirred solution of sodium periodate (3.4 g, 16 mmol) in water (25 mL) while maintaining the reaction temperature at 0 °C. The reaction was left an additional 20 min after which time sodium borohydride (2.0 g, excess) was added portionwise while again ensuring the reaction temperature was maintained at 0 °C. On complete addition the solid was filtered and washed with ethanol (50 mL), and the filtrate was concentrated in vacuo to afford a syrup. Chromatography afforded **7** (2.74 g, 92%) as a syrup. ¹H NMR δ 4.24 (m, 1H), 3.61 (m, 4H), 3.25 (m, 1H), 3.12 (m, 1H), 2.24 (m, 1H), 1.45 (s, 9H). ¹³C NMR δ 155.2, 80.2, (73.2, 72.4), 63.1, (53.1, 52.7), (48.6, 48.1), (47.0, 46.5), 28.9. HRMS (M^+) calcd for $\text{C}_{10}\text{H}_{20}\text{NO}_4$: 218.1392. Found 218.1392.

(3*R*,4*R*)-*N*-*tert*-Butoxycarbonyl-3-benzyloxy-4-benzyloxymethylpyrrolidine (**8**). Sodium hydride (140 mg, 60% oil dispersion, 3.7 mmol) was added portionwise to a stirred solution of benzyl bromide (300 μL , 2.8 mmol) and **7** (200 mg, 0.92 mmol) in DMF (10 mL) at 0 °C. On complete addition, the resulting suspension was allowed to warm to room temp, diluted with toluene (100 mL), washed with water (50 mL) and brine (50 mL), dried (MgSO_4), and concentrated in vacuo to afford a syrup. Chromatography afforded **8** (350 mg, 96%) as an oil, which was used in the next step without purification.

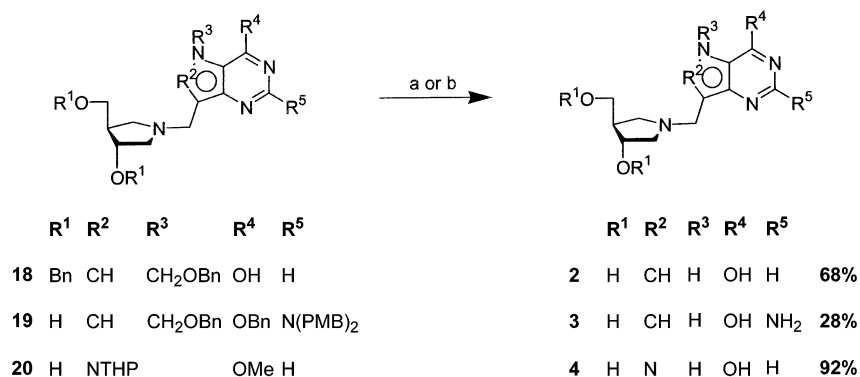
(3*R*,4*R*)-3-Benzyloxy-4-benzyloxymethylpyrrolidine Hydrochloride (**9**). Hydrochloric acid (2 mL, 1 M) was added to a solution of **8** (500 mg, 1.3 mmol) in methanol (2 mL) and the resulting mixture stirred for 1 h at 40 °C. On completion the reaction was concentrated in vacuo to afford **9** as the hydrochloride salt (370 mg, 100%). ¹H NMR δ 7.35-7.21 (m, 10H), 4.48 (m, 4H), 4.08 (d, J = 2.9 Hz, 1H), 3.53 (m, 1H), 3.44 (m, 3H), 3.24 (m, 1H), 2.65 (m, 1H). ¹³C NMR δ 138.0, 137.6, 128.9, 128.8, 128.3, 128.2, 79.3, 73.7, 71.9, 68.7, 49.6, 46.4, 44.8.

(3*R*,4*R*)-3-Hydroxy-4-hydroxymethylpyrrolidine Hydrochloride (**1-HCl**). Hydrochloric acid (5 mL, 12 M) was added dropwise to a stirred solution of **7** (2.3 g, 10.6 mmol) in methanol (5 mL) at room temperature. After 1 h the reaction was concentrated in vacuo to afford **1-HCl** (1.63 g, 100%) as an oil. ¹H NMR δ 4.43 (quintet, J = 3.0 Hz, 1H), 3.46 (dd, J = 12.7, 5.1 Hz, 1H), 3.29 (dd, J = 12.7, 2.2 Hz, 1H), (m, 1H), 3.18 (dd, J = 12.3, 5.8 Hz, 1H), 2.49 (m, 1H). ¹³C NMR δ 71.9, 60.9, 52.1, 47.9, 46.6. ¹H and ¹³C NMR of the free base were identical to those reported in the literature.²⁵

7-Benzyloxymethyl-6-*O*-*tert*-butyl-9-deaza-9-formylhypoxanthine (**14**). 7-Benzyloxymethyl-9-bromo-6-*O*-*tert*-butyl-9-deaza-hypoxanthine¹⁵ (**11**) (400 mg, 1.02 mmol) was dissolved in diethyl ether (10 mL) and anisole (5 mL) and cooled to -78 °C. *n*-Butyllithium (600 μL , 2.5 M) was then added dropwise at such a rate as to maintain the reaction temper-

Scheme 4^a

^a Reagents: (a) NaCNBH₃, MeOH, room temp.. (b) TFA, DCM, room temp.

Scheme 5^a

^a Reagents: (a) HCl, MeOH; (b) i, TFA, DCM; ii, H₂, Pd(OH)₂, EtOH.

Table 1. Inhibition Constants for the Interaction of Immucillins with Human PNP

inhibitor	human PNP ^a	
	K _i (pM)	K _i [*] (pM)
Immucillin-H	3300 ± 200	56 ± 15
Immucillin-G	540 ± 100	42 ± 6
8-Aza-Immucillin-H	1400 ± 200	180 ± 20
DADMe-ImmH 2	1100 ± 120	16 ± 1.4
DADMe-ImmG 3	163 ± 25	6.8 ± 1.2
8-aza-DADMe-ImmH 4	2000 ± 50	no slow onset

^a K_i^{*} is the dissociation constant for E + I ⇌ EI^{*}.

ature below -70°C and the resulting solution left for 30 min at -78°C . Dimethylformamide (100 μL) was then added, and the reaction was left stirring for an additional 30 min and then quenched with water and allowed to warm to room temp. The reaction was diluted with ethyl acetate (100 mL), washed with water (30 mL) and brine (30 mL), dried (MgSO₄), and concentrated in vacuo to afford a syrup. Purification by chromatography afforded **14** (270 mg, 78%) as a solid. Mp 100–101 $^{\circ}\text{C}$. ¹H NMR δ 10.29 (s, 1H), 8.62 (s, 1H), 7.98 (s, 1H), 7.34–7.22 (m, 5H), 5.79 (s, 2H), 4.53 (s, 2H), 1.71 (s, 9H). ¹³C NMR δ 184.8, 156.63, 152.6, 150.0, 136.7, 136.6, 128.9, 128.5, 127.8, 118.4, 84.4, 78.3, 71.0, 29.0. HRMS (MH⁺) calcd for C₁₉H₂₁N₃O₃: 340.1661. Found 340.1652.

7-Benzyloxymethyl-6-O-benzyl-9-deaza-9-formyl-2-N-bis(4-methoxybenzyl)guanine (15). *n*-Butyllithium (0.5 mL, 1.5 M) was added dropwise to a stirred solution of 7-benzyloxymethyl-6-O-benzyl-9-bromo-9-deaza-2-N-bis(4-methoxybenzyl)guanine²⁹ (**12**) in diethyl ether (6 mL) and anisole (3 mL) at -80°C under an inert atmosphere. The reaction was stirred for an additional 30 min at -80°C , and then DMF (1.0 mL) was added and the reaction was allowed to warm to room temp. The reaction was quenched with water (50 mL) and extracted with chloroform (2 \times 100 mL). The organic

layers were combined, washed with brine, dried (MgSO₄), filtered, and concentrated in vacuo to afford a solid residue. The solid was triturated with ethanol to afford **15** (280 mg, 72%) as a white solid. Mp 172–174 $^{\circ}\text{C}$. ¹H NMR δ 10.25 (s, 1H), 7.79 (s, 1H), 7.30–7.21 (m, 13H), 6.85–6.82 (m, 5H), 5.62 (s, 2H), 5.44 (s, 2H), 4.84 (s, 4H), 4.45 (s, 2H), 3.79 (s, 6H). ¹³C NMR δ 185.5, 159.4, 159.1, 156.5, 153.9, 136.9, 136.7, 134.9, 131.5, 129.5, 128.9, 128.5, 128.3, 128.0, 117.3, 114.2, 111.0, 78.4, 71.0, 67.9, 55.7, 49.5. HRMS (MH⁺) calcd for C₃₈H₃₇N₄O₅: 629.2764. Found 629.2749.

8-Aza-9-deaza-9-formyl-6-O-methyl-8-tetrahydropyranylhypoxanthine (16). *n*-Butyllithium (0.7 mL, 2.4 M) was added dropwise to a stirred solution of 8-aza-9-bromo-9-deaza-6-O-methyl-8-*N*-tetrahydropyranylhypoxanthine³⁰ (**13**) (530 mg, 1.7 mmol) in THF (20 mL) at -78°C under an inert atmosphere. The reaction was stirred for an additional 30 min at -78°C , and then DMF (1.0 mL) was added and the reaction was allowed to warm to room temp. The reaction was quenched with water (50 mL) and extracted with toluene (2 \times 100 mL). The organic layers were combined, washed with brine, dried (MgSO₄), filtered, and concentrated in vacuo to afford a solid residue. Chromatography afforded **16** as a solid. ¹H NMR δ 10.43 (s, 1H), 8.71 (s, 1H), 6.55 (dd, J = 10.0, 2.7 Hz, 1H), 4.25 (s, 3H), 4.13 (m, 1H), 3.83 (dt, J = 10.8, 2.8 Hz), 2.53–1.65 (m, 7H). ¹³C NMR δ 177.0, 161.5, 154.5, 143.9, 130.2, 128.9, 87.0, 67.4, 53.5, 28.7, 23.7, 21.2. HRMS (M⁺) calcd for C₁₂H₁₄N₄O₃: 262.1066. Found 262.1068.

(3*R*,4*R*)-1-[(7-Benzyloxymethyl-9-deazahypoxanthin-9-yl)methyl]-3-benzyloxy-4-benzyloxymethylpyrrolidine (18). Sodium cyanoborohydride (100 mg, 1.59 mmol) was added to a stirred solution of **14** (220 mg, 0.64 mmol) and **9**-HCl (190 mg, 0.57 mmol) in methanol (5 mL) which was stirred overnight at room temp. The reaction was then concentrated in vacuo to afford **17** as a syrup, which was not further characterized. The syrup was redissolved in DCM (2 mL) and TFA (0.5 mL) was added. The resulting solution was stirred

for 1 h at room temp and then concentrated in vacuo to afford a solid residue, which was redissolved in water. The aqueous phase was washed with DCM ($\times 2$) and concentrated in vacuo. Chromatography of the resulting residue afforded **18** (202 mg, 63%) as a solid. $^1\text{H NMR}$ δ 7.87 (1H, s), 7.32 (1H, s), 7.31–7.23 (m, 5H), 5.89 (s, 2H), 4.56 (s, 2H), 4.50 (s, 2H), 4.48 (s, 2H), 4.47 (s, 2H), 3.87 (m, 2H), 3.81 (q, $J = 13.4$ Hz, 2H), 3.43 (d, $J = 7.1$ Hz, 2H), 3.01 (t, $J = 8.1$ Hz, 1H), 2.79 (d, $J = 4.7$ Hz, 1H), 2.55 (m, 1H), 2.36 (m, 1H). $^{13}\text{C NMR}$ δ 156.2, 145.8, 141.8, 138.9, 138.8, 137.6, 131.4, 128.8, 128.7, 128.7, 128.3, 128.2, 128.1, 128.0, 128.8, 117.9, 115.7, 81.3, 77.1, 73.5, 72.1, 71.4, 70.8, 60.0, 56.4, 48.6, 45.9. HRMS (MH⁺) calcd for $\text{C}_{34}\text{H}_{37}\text{N}_4\text{O}_4$: 565.2815. Found 565.2799.

(3R,4R)-1-[(9-deazahypoxanthin-9-yl)methyl]-3-hydroxy-4-hydroxymethylpyrrolidine (2). Compound **18** (120 mg, 0.21 mmol) and Pearlman's catalyst (120 mg, 20% Pd(OH)₂ on C) were suspended in ethanol (3 mL) and acetic acid (1 mL) and vigorously stirred under an atmosphere of hydrogen for 24 h at r.t.. The reaction was then filtered through Celite and concentrated in vacuo to afford a solid, which was redissolved in 7N methanolic ammonia, allowed to stand at room temp. for 1 h and then concentrated in vacuo. Chromatography and ion exchange of the resulting residue afforded **2** (38 mg, 68%) as a white solid with mp 248–250 °C. $^1\text{H NMR}$ δ 7.81 (s, 1H), 7.34 (s, 1H), 3.97 (brs, 1H), 3.65 (s, 2H), 3.53 (m, 1H), 3.44 (m, 1H), 2.93 (t, $J = 9.0$ Hz, 1H), 2.77 (m, 1H), 2.60 (1H, m), 2.33 (t, $J = 7.1$ Hz, 1H), 2.12 (brs, 1H). $^{13}\text{C NMR}$ δ 155.8, 144.1, 142.8, 130.0, 117.3, 111.1, 72.9, 62.7, 60.2, 54.8, 48.9, 47.3. HRMS (MH⁺) calcd for $\text{C}_{12}\text{H}_{16}\text{N}_4\text{O}_3$: 265.1301. Found 265.1302. Anal. Calc. ($\text{C}_{12}\text{H}_{16}\text{N}_4\text{O}_3 \cdot \frac{1}{2}\text{H}_2\text{O}$) C, H, N.

(3R,4R)-1-[[6-O-Benzyl-7-benzyloxymethyl-9-deaza-2-bis(4-methoxybenzyl)guanin-9-yl]methyl]-3-hydroxy-4-hydroxymethylpyrrolidine (19). Sodium cyanoborohydride (200 mg, 3.0 mmol) was added to a stirred solution of **15** (530 mg, 0.84 mmol) and 1·HCl (163 mg, 1.06 mmol) in methanol (10 mL) and the mixture was then stirred overnight at room temp.. The reaction mixture was absorbed onto silica and concentrated in vacuo. Chromatography of the resulting residue afforded **19** (430 mg, 70%) as a white solid. Mp 98–100 °C. $^1\text{H NMR}$ 7.49 (s, 1H), 7.35–7.12 (s, 14H), 6.81 (d, $J = 8.5$ Hz, 4H), 5.59 (s, 2H), 5.47 (s, 2H), 4.85–4.73 (m, 4H), 4.44 (s, 2H), 4.23–4.12 (m, 3H), 3.75 (s, 6H), 3.50–3.35 (m, 3H), 3.20 (dd, $J = 12.0, 5.0$ Hz, 1H), 3.08 (d, $J = 12.0$ Hz, 1H), 2.95 (dd, $J = 11.4, 5.4$ Hz, 1H), 2.24 (brs, 1H). $^{13}\text{C NMR}$ δ 159.0, 158.4, 156.7, 153.1, 137.6, 137.0, 135.0, 131.5, 129.4, 128.9, 128.7, 128.4, 128.3, 128.1, 128.0, 125.7, 114.3, 110.6, 105.1, 78.1, 73.1, 70.8, 68.0, 62.2, 60.7, 55.7, 54.8, 49.2, 48.9. HRMS (MH⁺) calcd for $\text{C}_{43}\text{H}_{48}\text{N}_5\text{O}_6$: 730.3605. Found 730.3629.

(3R,4R)-1-[[9-deazaguanin-9-yl]methyl]-3-hydroxy-4-hydroxymethylpyrrolidine (3). cHCl (2 mL) was added dropwise to a solution of **19** (370 mg, 0.5 mmol) in methanol (4 mL) and the resulting solution heated at reflux for 4 h. The reaction was cooled to room temp and then concentrated in vacuo. The resulting residue was partitioned between water and chloroform and separated and the water layer concentrated in vacuo. Silica gel and ion exchange chromatography of the resulting residue afforded **3** (39 mg, 28%) as a white solid. Mp 223–225 °C. $^1\text{H NMR}$ δ 7.18 (s, 1H), 4.03–3.98 (m, 1H), 3.58 (s, 2H), 3.55 (dd, $J = 11.1, 6.3$ Hz, 1H), 3.45 (dd, $J = 11.1, 7.4$ Hz, 1H), 2.97 (dd, $J = 10.0, 8.5$ Hz, 1H), 2.79 (dd, $J = 10.9, 6.3$ Hz, 1H), 2.64 (dd, $J = 10.9, 4.0$ Hz, 1H), 2.35 (dd, $J = 10.3, 7.0$ Hz, 1H), 2.20–2.09 (m, 1H). $^{13}\text{C NMR}$ δ 158.6, 152.8, 143.5, 129.6, 112.7, 107.9, 72.8, 62.6, 60.2, 54.8, 48.9, 47.8. HRMS (MH⁺) calcd for $\text{C}_{12}\text{H}_{18}\text{N}_5\text{O}_3$: 280.1410. Found 280.1413. Anal. ($\text{C}_{12}\text{H}_{17}\text{N}_5\text{O}_3 \cdot \frac{1}{2}\text{H}_2\text{O}$) C, H, N.

(3R,4R)-1-[(8-Aza-9-deaza-6-O-methyl-8-tetrahydropyran-9-yl)methyl]-3-hydroxy-4-hydroxymethylpyrrolidine (20). Sodium cyanoborohydride (100 mg, 1.59 mmol) was added to a stirred solution of **16** (340 mg, 1.3 mmol) and 1·HCl (190 mg, 0.57 mmol) in methanol (5 mL), and the mixture was stirred overnight at room temp. The reaction mixture was absorbed onto silica and concentrated in vacuo. Chromatography of the resulting residue afforded **20** (150 mg, 35%) as a syrup. $^1\text{H NMR}$ δ 8.39 (s, 1H), 5.90 (d,

$J = 9.1$ Hz, 1H), 4.17–3.94 (m, 4H), 4.12 (s, 3H), 3.67–3.52 (m, 2H), 2.94–2.79 (m, 2H), 2.66–2.52 (m, 2H), 2.35–2.09 (m, 2H), 1.70–1.56 (m, 2H). $^{13}\text{C NMR}$ δ 162.6, 152.2, (140.1, 140.0), 133.5, 131.6, (87.0, 86.9), 74.3, (68.3, 68.2), (64.3, 64.2), 62.6, (56.2, 56.1), 54.5, (50.6, 50.7), (47.7, 47.6), 29.7, 25.2, 21.8. HRMS (MH⁺) calcd for $\text{C}_{17}\text{H}_{25}\text{N}_5\text{O}_4$: 364.1985. Found 364.1982.

(3R,4R)-1-[(8-Aza-9-deazahypoxanthin-9-yl)methyl]-3-hydroxy-4-hydroxymethylpyrrolidine (4). Concentrated hydrochloric acid (1 mL, 12 M) was added to a solution of **20** (50 mg, 0.14 mmol) in methanol. The solution was stirred overnight and then concentrated in vacuo to afford a solid residue which was triturated with methanol and filtered to afford **4** (38 mg, 92%) as a solid. Mp 264–266 °C. $^1\text{H NMR}$ δ 8.13 (s, 1H), 4.35 (d, $J = 2.7$ Hz, 1H), 3.86 (m, 1H), 3.66–3.43 (m, 2H), 3.55 (d, $J = 5.7$ Hz, 2H), 3.10 (m, 1H), 2.44 (brs, 1H). $^{13}\text{C NMR}$ δ 154.7, 145.4, 137.1, 134.7, 128.6, 71.4, 60.6, 60.6, 55.0, 48.0, 47.9. HRMS (MH⁺) calcd for $\text{C}_{11}\text{H}_{16}\text{N}_5\text{O}_3$: 266.1253. Found 266.1248. Anal. ($\text{C}_{11}\text{H}_{15}\text{N}_5\text{O}_3 \cdot \text{HCl}$) C, H, N, Cl.

Biology. Protein Preparation. Human PNP was recloned into T7/NT-TOPO vector and expressed in BL21(DE3) *E. coli*. (to be published elsewhere).

Determination of Kinetic and Inhibition Constants. Continuous assays for PNP coupled the production of hypoxanthine to uric acid by xanthine oxidase.⁷ PNP (1.4 nM) was added to inosine (1 mM) and xanthine oxidase (60 mU/mL) in 50 mM KPO₄ buffer pH 7.4 (25 °C). The increase in absorbance was monitored at 293 nm ($\epsilon_{293} = 12.9$ mM⁻¹). For K_i and K_i^* analysis, the amounts of enzyme and inhibitor were adjusted to give an absorbance change < 1.0 for the full analysis. Initial inhibition (K_i) was determined by fitting to the equation for competitive inhibition: $u_i = (k_{\text{cat}}S)/(K_m(1+I/K_i) + S)$, where u_i , k_{cat} , K_m , and K_i are initial rates, catalytic turnover, Michaelis constant, and inhibitor dissociation constant, respectively. The dissociation constant for tight bound complex (K_i^*) was determined by the same equation after the slow-onset equilibrium had been achieved. Valid analysis requires inhibitor to be present at $> 10\times$ enzyme concentration.³⁴ Inhibitor release studies used an inhibitor/enzyme subunit molar ratio of 1.10 and 1.09 for DADMe-ImmH and Immucillin-H, respectively. A solution of PNP (12.6 μL of 96 μM) was incubated 5.5 h (25 °C) with 105 μM Immucillin-H or 108 μM DADMe-Immucillin-H. The mixture was diluted 500 000 times, by adding 1 μL to 500 μL of 20 mM Tris HCl, pH = 7.5 buffer, and then 1 μL of this dilution was added directly to 1 mL of reaction mixture containing 18 mM inosine and 60 mU/mL xanthine oxidase in 50 mM KPO₄, pH = 7.5 buffer. The inhibitor release studies were performed in the absence and presence of phosphate at 50 mM.

Acknowledgment. This work was supported by research grant GM41916 from the NIH and by the New Zealand Foundation for Research, Science & Technology Contract.

References

- (1) Kline, P. C.; Schramm, V. L. Purine nucleoside phosphorylase. Inosine hydrolysis, tight binding of the hypoxanthine intermediate, and third-the-sites reactivity. *Biochemistry* **1992**, *31*, 5964–5973.
- (2) Kline, P. C.; Schramm, V. L. Purine Nucleoside Phosphorylase. Catalytic mechanism and transition state analysis of the arsenolysis reaction. *Biochemistry* **1993**, *32*, 13212–13219.
- (3) Kline, P. C.; Schramm, V. L. Pre-steady-state transition-state analysis of the hydrolytic reaction catalyzed by purine nucleoside phosphorylase. *Biochemistry* **1995**, *32*, 1153–1162.
- (4) Furneaux, R. H.; Limberg, G.; Tyler, P. C.; Schramm, V. L. Synthesis of transition state inhibitors for *N*-riboside hydrolases and transferases. *Tetrahedron* **1997**, *53*, 2915–2930.
- (5) Evans, G. B.; Furneaux, R. H.; Gainsford, G. J.; Schramm, V. L.; Tyler, P. C. Synthesis of transition state analogue inhibitors for purine nucleoside phosphorylase and *N*-riboside hydrolases. *Tetrahedron* **2000**, *56*, 3053–3062.
- (6) Evans, G. B.; Furneaux, R. H.; Hutchinson, T. L.; Kazar, H. S.; Morris, P. E., Jr.; Schramm, V. L.; Tyler, P. C. Addition of lithiated 9-deazapurine derivatives to a carbohydrate cyclic imine: Convergent synthesis of the aza-*C*-nucleoside immucillins. *J. Org. Chem.* **2001**, *66*, 5723–5730.

- (7) Miles, R. W.; Tyler, P. C.; Furneaux, R. H.; Bagdassarian, C. K.; Schramm, V. L. One-third-the-sites transition state inhibitors for purine nucleoside phosphorylase. *Biochemistry* **1998**, *37*, 8615–8621.
- (8) Miles, R. W.; Tyler, P. C.; Furneaux, R. H.; Bagdassarian, C. K.; Schramm, V. L. Purine nucleoside phosphorylase. Transition state structure, transition state inhibitors and one-third-the-sites reactivity. In *Enzymatic Mechanisms*. Edited by Frey, P. A., Northrop, D. B. IOS Press: Washington, DC, 1999; p 32–47.
- (9) Kicska, G. A.; Tyler, P. C.; Evans, G. B.; Furneaux, R. H.; Shi, W.; Fedorov, A.; Lewandowicz, A.; Cahill, S. M.; Almo, S. C.; Schramm, V. L. Atomic dissection of the hydrogen bond network for transition-state analogue binding to purine nucleoside phosphorylase. *Biochemistry* **2002**, *49*, 14489–14498.
- (10) Evans, G. B.; Furneaux, R. H.; Gainsford, G. J.; Hanson, J. C.; Kicska, G. A.; Sauve, A. A.; Schramm, V. L.; Tyler, P. C. 8-Aza-immucillins as transition-state analogue inhibitors of purine nucleoside phosphorylase and nucleoside hydrolases. *J. Med. Chem.* **2003**, *46*, 155–160.
- (11) Kicska, G. A.; Tyler, P. C.; Evans, G. B.; Furneaux, R. H.; Schramm, V. L.; Kim, K. *J. Biol. Chem.* **2002**, *277*, 3226–3231.
- (12) Kicska, G. A.; Tyler, P. C.; Evans, G. B.; Furneaux, R. H.; Kim, K.; Schramm, V. L. Transition state analogue inhibitors of purine nucleoside phosphorylase from *Plasmodium falciparum*. *J. Biol. Chem.*, **2002**, *277*, 3219–3225.
- (13) Basso, L. A.; Santos, D. S.; Shi, W.; Furneaux, R. H.; Tyler, P. C.; Schramm, V. L.; Blanchard, J. S. Purine nucleoside phosphorylase from *Mycobacterium tuberculosis*. Analysis of inhibition by a transition state analogue and dissection by parts. *Biochemistry* **2001**, *40*, 8196–8203.
- (14) Shi, W.; Basso, L. A.; Santos, D. S.; Tyler, P. C.; Furneaux, R. H.; Blanchard, J. S.; Almo, S. C.; Schramm, V. L. Structures of purine nucleoside phosphorylase from *Mycobacterium tuberculosis* in complexes with Immucillin-H and its pieces. *Biochemistry* **2001**, *40*, 8204–8215.
- (15) Evans, G. B.; Furneaux, R. H.; Lewandowicz, A.; Schramm, V. L.; Tyler, P. C. Exploring structure–activity relationships of transition state analogues of human purine nucleoside phosphorylase. *J. Med. Chem.* **2003**, *46*, 3412–3423.
- (16) Eriksson, S.; Thelander, L.; Kaerman, M. Allosteric regulation of calf thymus ribonucleoside diphosphate reductase. *Biochemistry* **1979**, *18*, 2948–2952.
- (17) Markert, M. L. Purine nucleoside phosphorylase deficiency. *Immunodef. Rev.* **1991**, *3*, 45–81.
- (18) Montgomery, J. A. Purine Nucleoside Phosphorylase: A target for drug design. *Med. Res. Rev.* **1993**, *13*, 209–228.
- (19) Sircar, J. C.; Gilbertsen, R. B. Purine nucleoside phosphorylase (PNP) inhibitors: Potentially selective immunosuppressive agents. *Drugs Future* **1988**, *13*, 653–668.
- (20) Bantia, S.; Ananth, S. L.; Parker, C. D.; Horn, L. L.; Upshaw, R. Mechanism of inhibition of T-acute lymphoblastic leukemia cells by PNP inhibitor-BCX-1777. *Int. Immunopharmacol.* **2003**, *3*, 879.
- (21) Lewandowicz, A.; Shi, W.; Evans, G. B.; Tyler, P. C.; Furneaux, R. H.; Basso, L. A.; Santos, D. S.; Almo, S. C.; Schramm, V. L. Over-the-barrier transition state analogues and crystal structure with *Mycobacterium Tuberculosis* purine nucleoside phosphorylase. *Biochemistry* **2003**, *42*, 6057–6066.
- (22) Jaeger, E.; Biel, J. H. Pyrrolidinediols. 1-Substituted 3-hydroxymethyl-4-hydroxypyrrolidines and derivatives. *J. Org. Chem.* **1965**, *30*, 740–744.
- (23) Bols, M.; Hansen, S. U. 1-Azaribofuranoside analogues as designed inhibitors of purine nucleoside phosphorylase. Synthesis and biological evaluation. *Acta Chem. Scand.* **1998**, *52*, 1214–1222.
- (24) Ichikawa, Y.; Makino, K. Synthesis of a 2-deoxy-ribose type 1-N-aminosugar. *Tetrahedron Lett.* **1998**, *39*, 8245–8248.
- (25) Filichev, V. V.; Brandt, M.; Pedersen, E. B. Synthesis of an aza analogue of 2-deoxy-D-ribofuranose and its homologues. *Carbohydrate Res.* **2001**, *333*, 115–122.
- (26) Lim, M.-I.; Klein, R. S.; Fox, J. J. Synthesis of the pyrrolo[3,2-d]pyrimidine C-nucleoside isostere of inosine. *Tetrahedron Lett.* **1980**, *21*, 1013–1016.
- (27) Lim, M.-I.; Klein, R. S. Synthesis of “9-deazaadenosine”; A new cytotoxic C-nucleoside isostere of adenosine. *Tetrahedron Lett.* **1981**, *22*, 25–28.
- (28) Lim, M.-I.; Ren, W.-Y.; Otter, B. A.; Klein, R. S. Synthesis of “9-deazaguanosine” and other new pyrrolo[3,2-d]pyrimidine C-nucleosides. *J. Org. Chem.* **1983**, *48*, 780–788.
- (29) Evans, G. B.; Furneaux, R. H.; Hausler, H.; Larsen, J. S.; Tyler, P. C. Aza-C-nucleoside synthesis: heteroaryl lithium carbanion additions to a carbohydrate cyclic imine and nitron. Submitted for publication in *J. Org. Chem.*
- (30) Stone, T. E.; Eustace, E. J.; Pickering, M. V.; Doyle, D. G., Jr. Pyrazolo[4,3-d]pyrimidines. Regioselectivity of N-alkylation. Formation, rearrangement, and aldehyde coupling reactions of 3-lithio derivatives. *J. Org. Chem.* **1979**, *44*, 505–510.
- (31) Giblett, E. R.; Ammann, A. J.; Wara, D. W.; Sandman, R.; Diamond, L. K. Nucleoside-phosphorylase deficiency in a child with severely defective T-cell immunity and normal B-cell immunity. *Lancet* **1975**, *1*, 1010–1013.
- (32) Bantia, S.; Miller, P. J.; Parker, C. D.; Ananth, S. L.; Horn, L. L.; Babu, Y. S.; Sandhu, J. S. Comparison of in vivo efficacy of BCX-1777 and cyclosporin in xenogeneic graft-vs.-host disease: the role of dGTP in antiproliferative action of BCX-1777. *Int. Immunopharmacol.* **2002**, *2*, 913–23.
- (33) Kilpatrick, J. M.; Morris, P. E.; Serota, D. G.; Phillips, D.; Moore, D. R.; Bennett, J. C.; Babu, Y. S. Intravenous and oral pharmacokinetic study of BCX-1777, a novel purine nucleoside phosphorylase transition-state inhibitor. In vivo effects on blood 2'-deoxyguanosine in primates. *Int. Immunopharmacol.* **2003**, *3*, 541–548.
- (34) Morrison, J. F.; Walsh, C. T. The behavior and significance of slow-binding enzyme inhibitors. *Adv. Enzymol. Relat. Areas Mol. Biol.* **1988**, *61*, 201–301.

JM030305Z